Supporting Information

Mechanistic Kinetic Modeling of Thiol–Michael Addition Photopolymerizations *via* Photocaged 'Superbase' Generators: An Analytical Approach

Mauro Claudino[a], Xinpeng Zhang[a], Marvin D. Alim[a], Maciej Podgórski[b], and Christopher N. Bowman[a]

[a] Department of Chemical and Biological Engineering, University of Colorado, UCB 596, Boulder, CO 80309, USA.

[b] Faculty of Chemistry, Department of Polymer Chemistry, MCS University, pl. Marii Curie-Skłodowskiej 5, 20 – 031 Lublin, Poland.

I. Calculation of the photolysis *quantum yield* ϕ_λ (number of cleaved molecules of photobase per absorbed photon), associated with base generation:

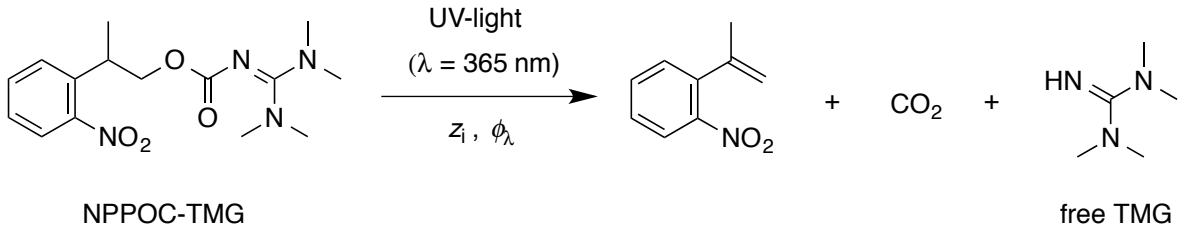

NPPOC-TMG free TMG

$$\phi_\lambda = \frac{rate\ of\ photobase\ generator\ consumed}{rate\ of\ photon\ absorption}$$

$$\ln\left(\frac{[\mathrm{PB}]_t}{[\mathrm{PB}]_0}\right) = -z_i t$$

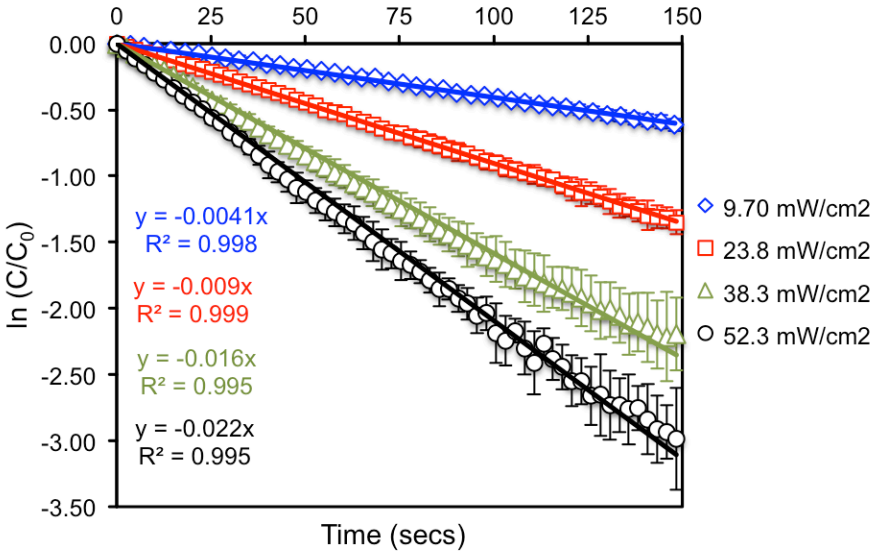

Figure S1. First-order photo-dissociation kinetics of NPPOC-TMG ($[PB]_0$ = 0.08 M, ~2.0 wt.%) in neat GDMP monomer at four different UV-light intensities (in mW/cm^2). Photo-cleavage of PB was recorded for 5-min of reaction, however only the first 2.5-min are reported; thereafter the kinetics started to deviate gradually from a first-order rate law. Standard deviations from three independent repeat measurements are shown.

$$z_i = \frac{\ln(10)\,\phi_\lambda\,\epsilon_\lambda\,\lambda}{N_{Av}\,h\,c}\cdot I_{inc}$$

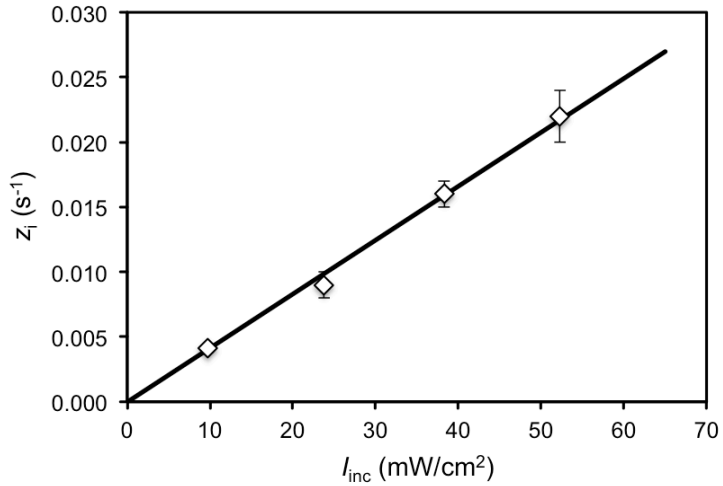

Figure S2. Linear correlation between z_i and light intensity: $z_i = 4.15\times10^{-4} \times I_{inc}$ (R^2 = 0.995). *Quantum yield*: $\phi_{365\ nm} = 0.24 \pm 0.01$.

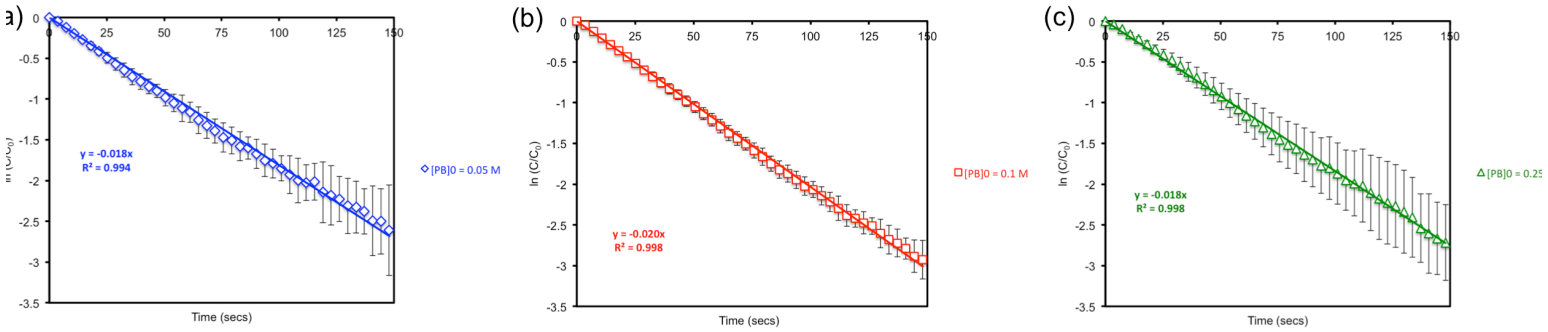

Figure S3. Unimolecular photo-dissociation kinetics of NPPOC-TMG in neat GDMP monomer at different initial concentrations of photobase, $[PB]_0$: (a) 0.05 M, (b) 0.1 M, and (c) 0.25 M. UV-light irradiance: I_{inc} = 63.1±2.3 mW/cm^2 (λ = 365 nm), $z_i(I_{inc})$ = 0.019±0.001 s^{-1}. *Quantum yield*: $\phi_{365\ nm}$ = 0.18 ± 0.01. Note that for a process that follows a first-order rate law the value of z_i is independent of the initial concentration of photobase, i.e., all initial rates extrapolate to a value of $t = 1/z_i$ in a concentration *vs*. time plot. The *quantum yield* returned using this method is very similar to that calculated from figure S2. Error bars represent standard deviations around the mean obtained from three independent kinetic runs. Differences observed in the slopes fall within experimental errors.

Note: Infrared (FT–IR) spectroscopy measurements were taken by monitoring in real-time the disappearance of the carbonyl peak of NPPOC-TMG (1600–1500 cm^{-1}) using liquid solution thin-films sandwiched between two potassium bromide (KBr) salt crystals.

II. Estimation of the kinetic parameters k_p and k_{CT} from data measured by Real-time Fourier Transform Infrared (RT-FTIR) Spectroscopy:

Experimental Methodology:
Liquid mixtures of ethylene glycol di(3-mercaptopropionate)/GDMP (dithiol) and ethyl vinyl-sulfone/EVS (monovinyl) supplemented with 2.0 wt.% of NPPOC-TMG were prepared and immediately deposited between two KBr salt plates prior to the acquisition of FT-IR spectral data. Each sample was placed horizontally in a Nicolet 6700 FT-IR spectroscopy optical bench combined with a vertical light cable. Each mixture was continuously irradiated at the surface of the sample with UV-light emitted from an EXFO Acticure 4000 high pressure mercury vapor short arc lamp equipped with a 365 narrow bandpass filter. The UV-irradiance delivered was measured using an International Light IL1400A handheld radiometer equipped with a GaAsP detector (model SEL005), a wide bandpass filter (model WBS302) and a quartz diffuser (model W). Kinetic measurements were conducted *in situ* by recording the progress of the photochemical reaction following the disappearance of thiol and vinyl-sulfone peaks located at 2560 cm^{-1} and 3050 cm^{-1}, respectively. All reactions were conducted under ambient conditions. Series scans were recorded with spectra collected at a rate of approximately five scans every two seconds. The FT-IR sample chamber was continuously purged with dry air. Conversions were

calculated using the ratio of peak areas to the peak area prior to the reaction. The observed kinetics was modeled analytically using the integrated form of equation (A1) derived from a basic mechanistic scheme proposed for the reaction. Reaction rate constants were estimated using the 'flooding' technique (~22-fold relative mole excess of thiol functionalities) in one occasion, providing reactions are carried out in the presence of enough thiol so that its concentration remains effectively constant, while performing the same reaction under equimolar conditions of functional groups in another occasion. An estimate for the *propagation/chain-transfer* rate constant quotient, $k_p/k_{CT} = 0.15$, was obtained by simultaneously fitting the detailed mechanism to measured kinetic data collected over a range of experimental conditions. For practical reasons only real-time data obtained with a relative excess of thiol is reported for the 'flooding' technique as reversing the procedure by increasing the vinyl-sulfone amount relative to that of the thiol, using the same factor, significantly diluted the thiol peak intensity under FT-IR spectroscopy to yield high noise kinetic data.

III. Linearized forms of the general mechanistic rate equation:

$$R_{rxn} = -\frac{d[x]_t}{dt} = k_{kin}[B]_t[x]_t \text{, with} \tag{A1}$$

$$k_{kin} = \frac{r_0 k_p k_{CT}}{k_p + r_0 k_{CT}} \qquad (\text{for } [x]_t = [C{=}C]_t) \tag{A2}$$

$$k_{kin} = \frac{k_p k_{CT}}{k_p + r_0 k_{CT}} \qquad (\text{for } [x]_t = [RSH]_t) \tag{A3}$$

allows extraction of the catalytic cycle rate constants, k_p and k_{CT}, individually *via* a single regression plot according to:

1. Linear plot of $1/k_{kin}$ *vs.* $1/r_0$ (from Eqn. (A2)):

$$\frac{1}{k_{kin}} = \left(\frac{1}{k_{CT}}\right)\frac{1}{r_0} + \frac{1}{k_p} \tag{B1}$$

with slope = $1/k_{CT}$ and intercept at origin = $1/k_p$.

2. Linear plot of r_0/k_{kin} *vs.* r_0 (from Eqn. (A2)):

$$\frac{r_0}{k_{kin}} = \left(\frac{1}{k_p}\right)r_0 + \frac{1}{k_{CT}} \tag{B2}$$

with slope = $1/k_p$ and intercept at origin = $1/k_{CT}$;

3. Linear plot of $1/k_{kin}$ *vs.* r_0 (from Eqn. (A3)):

$$\frac{1}{k_{kin}} = \left(\frac{1}{k_p}\right) r_0 + \frac{1}{k_{CT}} \tag{B3}$$

with slope = $1/k_p$ and intercept at origin = $1/k_{CT}$.

Please note that the regression parameters obtained after the linearization may not exactly match those obtained by fitting the model to experiment, as the linearization changes the metrics of the data space affecting the regression analysis by applying the method of least squares.

IV. Determination of empirical scaling exponents:

The apparent reaction orders, n and m, with respect to vinyl ($[C{=}C]_t$) and thiol ($[RSH]_t$) concentrations, respectively, represent individual mole fractions of the reactive anionic intermediates within the total anionic species in the reaction system. Therefore, making $n = [RS^-]_t / ([RS^-]_t + [RC^-]_t) = 1 / (1 + y)$ and $m = [RC^-]_t / ([RS^-]_t + [RC^-]_t) = y / (1 + y)$; i.e., $n + m = 1$ at $r_0 = 1$, yields $y = m/n = [RC^-]_t/[RS^-]_t = k_p/k_{CT}$. The value of y can be determined experimentally from the ratio of the conversion rates, R_t, taken at stoichiometries $r_0 \neq 1$ to that of $r_0 = 1$; i.e.,

$$R_t = \frac{R_{rxn}^{r_0 \neq 1}}{R_{rxn}^{r_0 = 1}} \tag{C1}$$

$$y = \frac{1 - r_0 R_t e^{-A \cdot F(t)}}{R_t e^{-A \cdot F(t)} - 1} \quad \text{for } r_0 < 1 \tag{C2}$$

$$y = \frac{r_0\left[1 - R_t e^{-B \cdot F(t)}\right]}{R_t e^{-B \cdot F(t)} - r_0} \quad \text{for } r_0 > 1 \tag{C3}$$

The time-dependent exponential term is described as:

$$F(t) = \frac{1 - e^{-z_i t}}{z_i} - t \tag{C4}$$

and the difference parameters for each stoichiometric regime given by:

$$A = \beta_{r_0<1} - \beta_{r_0=1} \tag{C5}$$

$$B = \beta_{r_0>1} - \beta_{r_0=1} \tag{C6}$$

At initial times, $t = 0$, all equations of y above are reduced to simple fractions involving $R_{t=0} = R_0$ and r_0. Replacing values of y in the original mole fractions allows quantifying n and m. Note that experimentally the individual reaction rates in eqn. (C1) should be treated as *average rates*, which can be estimated *via* linear regression of measured kinetic data (conversion *vs*. time profiles) within the same reaction period, Δt. Each experimental data segment yields a local slope equal to the average rate within this narrow interval having an average time t corresponding to the central value. Finally, by knowing n, m and, k_{kin} (obtained at $r_0 = 1$), one can then estimate k_p and k_{CT} since $k_p = k_{kin}/n$ and $k_{CT} = k_{kin}/m$.

Noticeably, when k_{kin} changes by variations in the reaction stoichiometry, r_0, the individual values of n and m also vary accordingly, although the ratio $y = m/n$ remains a fixed constant. Therefore, for kinetic experiments performed under off-stoichiometric conditions (i.e., $r_0 \neq 1$), the overall reaction order, $n + m = p$ (with $p \neq 1$), is determined by plotting $\ln(R_t)$ *vs*. $F(t)$ to yield $\Delta\beta = A$ (or B) as the slope and $\ln(p)$ the intercept at origin. The individual scaling exponents in these new conditions are now given by:

$$n = \frac{p-1}{1-r_0} \quad (\text{for } r_0 < 1) \tag{C7}$$

$$n = \frac{r_0-p}{r_0-1} \quad (\text{for } r_0 > 1) \tag{C8}$$

$$m = p - n \tag{C9}$$

Equivalently, equations (C2) and (C3) are expressed in terms of p, as:

$$y = \frac{1-r_0 p}{p-1} \quad (\text{for } r_0 < 1) \tag{C10}$$

$$y = \frac{r_0(p-1)}{r_0-p} \quad (\text{for } r_0 > 1) \tag{C11}$$

V. Derivation of the *induction time*, τ, expression:

When a bimolecular termination mechanism (Eqn. (D3)) is involved for the photo-generated base (B) by its preferential reaction with acidic impurities (HA), any amount of base produced is immediately neutralized before having the chance to react with the thiol (RSH) in step (2) of the reaction mechanism. Therefore, performing a general rate balance between the base produced and consumed *via* photolysis and acid-base neutralization, respectively, gives:

$$\left(\frac{d[\mathrm{B}]_t}{dt}\right)_{\text{overall}} = \left(\frac{d[\mathrm{B}]_t}{dt}\right)_{\text{initiation}} - \left(\frac{d[\mathrm{B}]_t}{dt}\right)_{\text{termination}} = f\, z_{\mathrm{i}}[\mathrm{PB}]_0 e^{-z_{\mathrm{i}}t} - k_{\mathrm{t}}[\mathrm{B}]_t[\mathrm{HA}]_t = 0 \tag{D1}$$

$$[\mathrm{HA}]_t = \frac{f\, z_{\mathrm{i}}[\mathrm{PB}]_0 e^{-z_{\mathrm{i}}t}}{k_{\mathrm{t}}[\mathrm{B}]_t} \tag{D2}$$

Since

$$\frac{d[\mathrm{HA}]_t}{dt} = -k_{\mathrm{t}}[\mathrm{B}]_t[\mathrm{HA}]_t \tag{D3}$$

by assuming $K'_{\mathrm{eq}} \gg 1$ in the acid-base neutralization equilibrium (with $K'_{\mathrm{eq}} > K_{\mathrm{eq}}$), and then replacing (D2) in (D3) yields the differential equation

$$\frac{d[\mathrm{HA}]_t}{dt} = -f\, z_{\mathrm{i}}[\mathrm{PB}]_0 e^{-z_{\mathrm{i}}t} \tag{D4}$$

Solving (D4) subjected to the initial conditions, $[\mathrm{HA}](0) = [\mathrm{HA}]_0$, affords the analytical solution describing the time development of $[\mathrm{HA}]_t$:

$$[\mathrm{HA}]_t = [\mathrm{HA}]_0 + f[\mathrm{PB}]_0\left(e^{-z_{\mathrm{i}}t} - 1\right) \tag{D5}$$

When $t = \tau$, the $[\mathrm{HA}]_{t=\tau} = 0$, and equation (D5) becomes

$$\tau = \frac{1}{z_{\mathrm{i}}}\ln\left(\frac{f[\mathrm{PB}]_0}{f[\mathrm{PB}]_0 - [\mathrm{HA}]_0}\right) \tag{D6}$$

Finally, equation (D6) can be expressed in terms of light intensity, by

$$\tau = \frac{1}{\varphi_i I_{inc}} \ln\left(\frac{f[PB]_0}{f[PB]_0 - [HA]_0}\right) \quad \text{(D7)}$$

VI. Thiol–ene reaction mechanism:

Initiation:

(1) $PI + h\nu \xrightarrow{z_i} In^{\bullet}$ (photolysis of initiator)

(2) $In^{\bullet} + RSH \xrightarrow{k_H} RS^{\bullet} + InH$ (hydrogen-transfer)

Propagation/chain-transfer:

(3) $RS^{\bullet} + C{=}C \xrightarrow{k_p} RC^{\bullet}$ (propagation)

(4) $RC^{\bullet} + RSH \xrightarrow{k_{CT}} P + RS^{\bullet}$ (chain-transfer)

Termination:

(5) $2\,RS^{\bullet} \xrightarrow{k_{t1}} RSSR$ (thiyl radical self-termination)

(6) $RS^{\bullet} + RC^{\bullet} \xrightarrow{k_{t2}} RSCR$ (cross-termination)

(7) $2\,RC^{\bullet} \xrightarrow{k_{t3}} RCCR$ (carbon radical self-termination)

Scheme S1. Thiol–ene mechanistic scheme used in the numerical simulations *via* COPASI. All radical-radical (re)combinations for termination are assumed to be equally likely—i.e., the bimolecular termination rate constants are all equivalent: $k_t = k_{t1} = k_{t2} = k_{t3}$ (in $M^{-1}s^{-1}$). $In^{\bullet}$ is designated a general carbon-centered radical fragment resulting from photo-cleavage of a generic radical photoinitiator (PI).

VII. Effect of the extent of inhibition χ on the reaction kinetics of photo-induced thiol–Michael addition polymerizations involving a strong base catalyst:

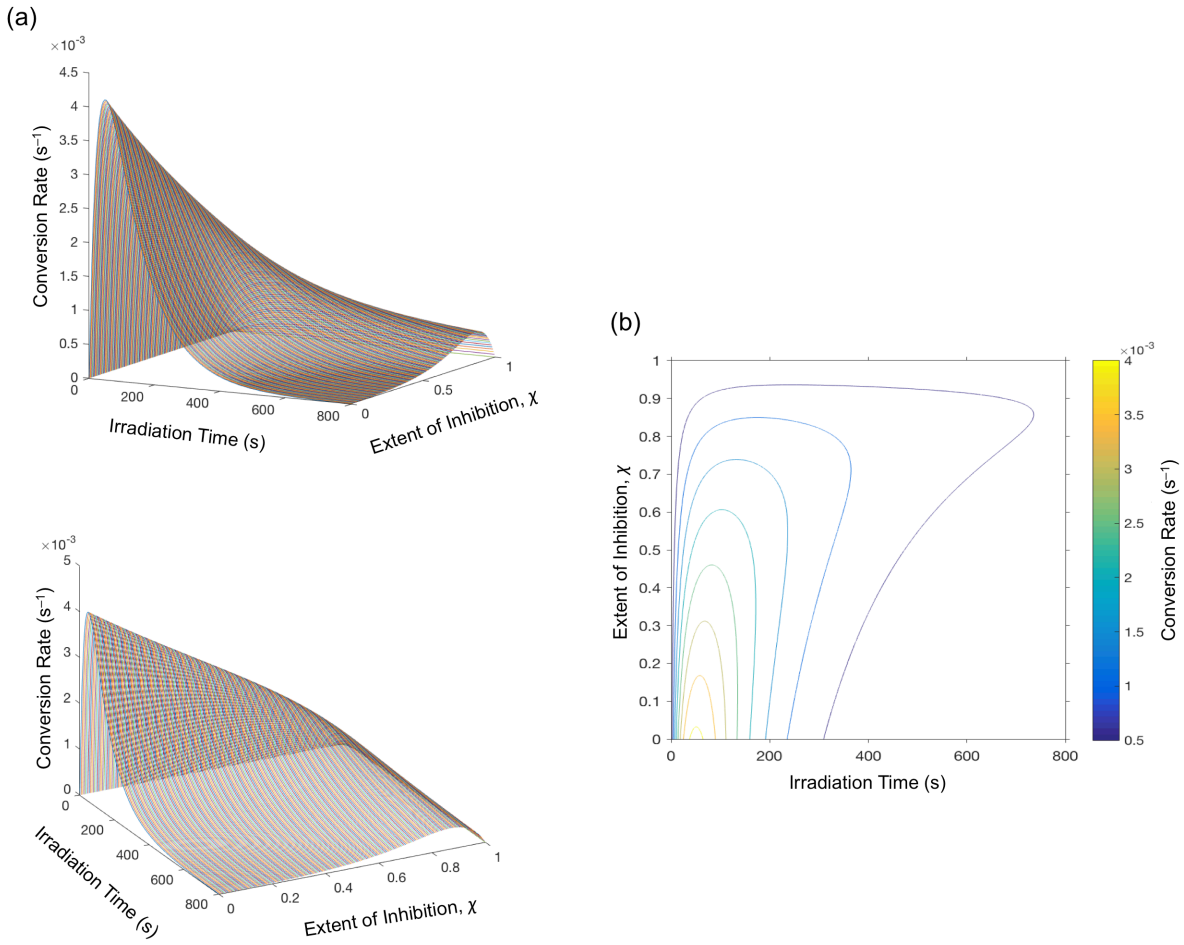

Figure S4. Stacked waterfall plots (a) and corresponding contour plot (b) showing the evolution of the thiol–Michael conversion rate with time and extent of inhibition.